

**Programmable self-assembly of diamond polymorphs from chromatic patchy particles**Niladri Patra<sup>1</sup> and Alexei V. Tkachenko<sup>2,\*</sup><sup>1</sup>*Department of Applied Chemistry, Indian Institute of Technology (Indian School of Mines), Dhanbad, Dhanbad 826004, India*<sup>2</sup>*Center for Functional Nanomaterials, Brookhaven National Laboratory, Upton, New York 11973, USA*

(Received 19 June 2018; published 26 September 2018)

We present a method of controlling polymorphism in self-assembly and apply it to the long-standing problem of assembly of a colloidal diamond. The latter is often viewed as the “holy grail” of the self-assembly field, due to the challenge that it presents as well as thanks to its potential as a step towards manufacturing of photonic band-gap materials. In our approach, we use a “chromatic” version of traditional building blocks, the so-called patchy particle. Namely, the individual patches that belong to the same particle in our model are distinguishable (“colored”) and their pairwise interactions are color dependent, which could be implemented with the help of DNA fictionalization. We propose a design procedure and verify it with the help of Brownian dynamics simulations. Not only are we able to “program” the self-assembly of a high-quality cubic diamond lattice, but a small modification of the coloring scheme also allows us to “reprogram” the system to assemble into the alternative polymorph, a hexagonal diamond.

DOI: [10.1103/PhysRevE.98.032611](https://doi.org/10.1103/PhysRevE.98.032611)**I. INTRODUCTION**

Programmable self-assembly is an emerging field in which desired morphologies are typically encoded by controlling interactions of constituent particles. It shows a great potential at various length scales, from nanometers to microns, and for a variety of physical realizations. Among the key ideas in the field are the use of molecular recognition, and anisotropic interactions between the building blocks. The two classes of model systems that best represent each of the two approaches are particles with DNA-mediated interactions [1–7], and patchy colloids [8–13]. While significant progress has been made within each of the two strategies, it is becoming increasingly clear that their combination has especially high potential for morphological control [14–18]. In this paper we demonstrate, with the help of Brownian dynamics simulations, that a hybrid approach based on patchy particles with distinguishable patches and type-dependent (“chromatic”) interactions [17,19] can be programmed to self-assemble into a specific desired superlattice among several polymorphs. Specifically, our model system deals with one of the most iconic and challenging structures in the field of self-assembly, i.e., the diamond lattice. It is often considered the “holy grail” of colloidal self-assembly due to its potential for fabrication of photonic band-gap materials [20–22].

In a diamond, each particle is supposed to be bound to four other particles forming a tetrahedron around it. A particle with a tetrahedral arrangement of patches is thought to be a natural building block that would favor a diamond lattice. The patchy particle model, originally proposed as a “primitive model” for associated liquids such as water [23], has gained substantial popularity in the past decade due to progress in colloidal science [8,9,13,24]. Initial interest in this class of systems was

sparked by their unusual phase behavior in the liquid regime, featuring “empty liquids,” reentrant regimes, and liquid-liquid coexistence [11,25–28]. More recently, the goal has shifted towards the use of patchy particles for self-assembly of crystalline phases [10,29–35], with diamond attracting a special interest.

Both Monte Carlo (MC) and molecular dynamics (MD) simulations of patchy particles with tetrahedral symmetry reveal serious fundamental limitations in their ability to form a diamond structure [10,19,32,34]. First, there are two forms of the diamond lattices, cubic diamond (CD) and hexagonal diamond (HD), both having local tetrahedral arrangement, as shown in Figs. 1(a) and 1(b). In addition, the CD lattice has to compete against a disordered structure, the so-called tetrahedral liquid. It is predicted that CD becomes a ground state of the patchy particle system only in the limit of sufficiently small patch size [32], i.e., very strong directionality of the bonds. Furthermore, even if the structure is favored thermodynamically, the existence of competing polymorphs results in prohibitively slow kinetics. Nevertheless, MD simulations show that CD becomes kinetically accessible if patch-patch interactions could couple the torsional degrees of freedom of the particles [33]. A specific implementation of such a coupling was proposed in Ref. [31]. In those simulations, both CD and HD lattices were successfully self-assembled from model colloids with noncircular, triangular-shaped patches.

There have been two recent reports of successful experimental realizations of diamond-related lattices. In one of them, realized at the nanoscale, DNA-functionalized nanoparticles (NPs) were combined with tetrahedral “DNA cages” [36]. However, the approach cannot be easily applied to other systems, such as micron-scale colloids, since the mechanism is very system specific. In another experiment, a double diamond structure was formed in a binary system of DNA-functionalized colloids, which can in principle be converted to a CD lattice [37]. The mechanism of its formation is

\*oleksiyt@bnl.gov

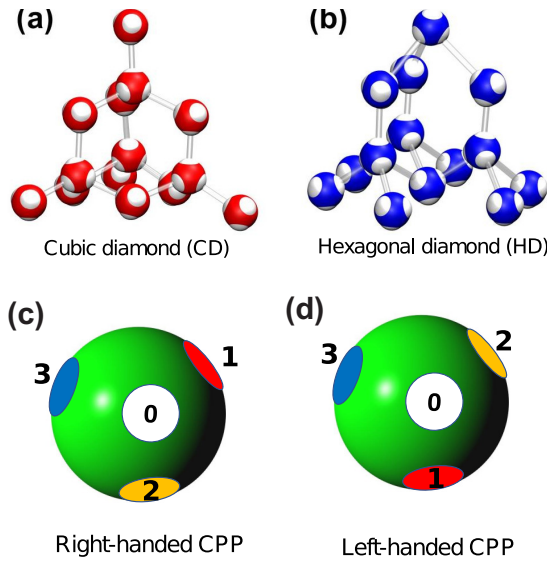


FIG. 1. Fragments of (a) cubic and (b) hexagonal diamond lattices. (c), (d) Chromatic patchy particles (CPPs) with tetrahedral patch arrangement. For four distinct colors of patches, there are two nonequivalent CPP types with opposite chiralities, called (c) right handed and (d) left handed here.

poorly understood. Conceptually, this approach is similar to an earlier proposed scenario of diamond manufacturing from a self-assembled Laves structure [38,39].

## II. CHROMATIC INTERACTIONS

In this paper, we demonstrate that one can preprogram the self-assembly of either of the diamond polymorphs, cubic or hexagonal, by using appropriate “coloring” of the chromatic patchy particles. The desired structure is of an exceptional quality and is formed in a robust manner for a wide range of the system parameters. Classical patchy particles have a number of chemically distinct patches placed on their surfaces in a particular manner, e.g., forming a tetrahedral pattern. Typically, all the patches are identical and have the same attractive interactions between them. We are using the term chromatic patchy particles (CPPs) [19] to denote a broad class of building blocks in which each patch may have of a distinct type (color), thus allowing for color-dependent interactions between them [see Figs. 1(c) and 1(d)].

Originally, the selectivity of patch-patch interactions was introduced in the context of controlling the phase behavior in the empty liquid regime [27,28]. More recently, inspired by the successful use of DNA-based binding, chromatic interactions were employed in numerical studies of programmable self-assembly of mesoscopic structures [15,18,40]. When it comes to their experimental implementation, the most natural way is to use DNA to “color” individual patches, and to rely on Watson-Crick hybridization for color-dependent interactions. In fact, one of the early numerical studies of chromatic patchy particles [17,18] was used to model the “DNA brick” technology (which does not involve any physical particles at all) [41]. More recently, CPP-like nanoblocks have been implemented with the help of the DNA origami technique,

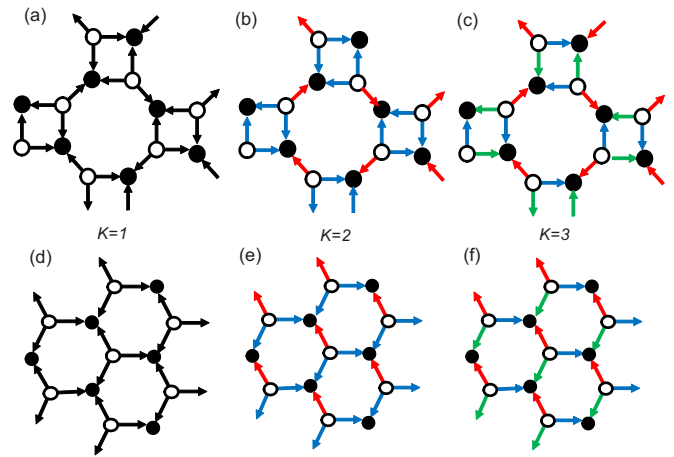


FIG. 2. Illustration of the concept of minimal coloring for the case of two-dimensional (2D) assembly of threefold patchy particles. (a)–(c) A so-called 4-8 lattice and (d)–(f) a honeycomb lattice, for bond types 1, 2, and 3, respectively. The number of particle types is  $N = 2$  in all cases, but the number of distinct patch-patch bonds,  $K$ , changes from 1 to 3.

by trapping NPs inside a DNA cage or frame with distinct single-stranded DNA terminals that play the role of patches [16,36,42]. Alternative technology involves “imprinting” a NP with a certain DNA pattern, with the help of a DNA origami scaffold [43]. Ironically, progress at the nanoscale has surpassed the advance in bigger, micron-scale colloids. While patchy colloids have been successfully decorated with DNA, this has been done so far in a non-patch-specific manner [9,44]. Still, the availability of such building blocks in the near future is very likely [24].

To understand how coloring can be used for programming a specific morphology, consider two two-dimensional (2D) structures shown in Fig. 2: the honeycomb and the “4-8” lattices. In both cases, each particle has three nearest neighbors, so it is natural to use three-patch particles as building blocks. The local geometry is slightly different for the two networks: in the honeycomb, the three bonds are oriented at  $120^\circ$  to each other, while in the 4-8 lattice, the angles are  $90^\circ$ ,  $135^\circ$ , and  $135^\circ$ . Nevertheless, this geometric distinction is too subtle to control the structure: one would need to use interactions with extremely well-defined bond orientations. Instead, one can introduce chromatic interactions to select one of the two polymorphs. We consider the system made of two particle types (black and white) and gradually increase its complexity by changing the number of distinct patches and/or bonds. Since DNA is the most natural mediator of chromatic patch-patch interactions, each bond in our model connects a pair of mutually complementary patches. In Fig. 2 the bonds are represented by arrows and their colors correspond to bond types (e.g., to particular pairs of complementary DNA sequences).

If all bonds are identical [Figs. 2(a) and 2(d)], the interaction rules cannot distinguish between the two potential structures. The same is true when the number of bond types,  $K$ , is increased to 2 [Figs. 2(b) and 2(e)]. However, for  $K = 3$  the two competing morphologies would require different designs of the building particles. Specifically, if black and

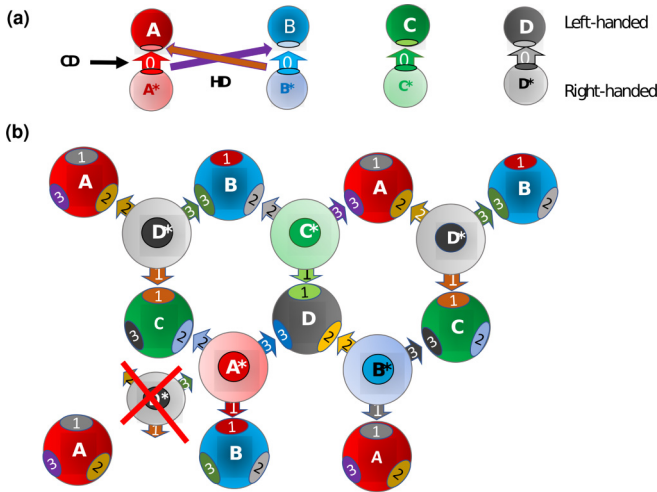


FIG. 3. Schematic representation of the coloring scheme used to encode CD and HD structures. It has  $N = 8$  particle types, and  $K = 16$  bond types: (a) four of them strong, (b) others weak.

white particles have the same chirality, one can only arrange them into a honetcomb, rather than a 4-8 lattice. Chirality here refers to the order of red, green, and blue patches on a 2D particle (we assume that the particle cannot be flipped to reverse this order). Interestingly, designing the black and white particles to have opposite chiralities *does not select* the 4-8 polymorph. The honeycomb would be a plausible structure for the heterochiral system as well (some particles would have to be rotated by  $120^\circ$  in that case). This simple 2D example gives a flavor of what we intend to achieve in this work. Our task, however, is more challenging. First, we will work in three dimensions, trying to select among the two structures, hexagonal and cubic diamond, that are *geometrically identical* at the nearest-neighbor level. Second, we are looking for a scheme that is immune to kinetic traps, thus leading to a robust and essentially error-free assembly of the desired structure. Finally, rather than selecting only one of the structures (e.g., CD), we are seeking a general method that can program assembly of either of the two polymorphs on demand.

### III. SYSTEM DESIGN

We have followed a coloring procedure from the previous section for the case of a CD lattice. As a result, we identified a coloring scheme that allows us to differentiate CD and HD structures and, furthermore, only allows binding of new particles in a way which is consistent with the target lattice. It requires eight distinct particle types with a maximum number of patch colors (four per particle). The 16 pairs of patches correspond to 16 distinct bonds. Our design is schematically represented in Fig. 3. We arranged the eight particle types into two groups:  $A, B, C, D$  and  $A^*, B^*, C^*, D^*$ . Each particle has four patches, 0, 1, 2, and 3, arranged in a left-handed manner for the first group, and a right-handed manner for the other [chirality is defined as in Figs. 1(d) and 1(e)]. We use a hierarchic approach, by making one of the bonds for each particle stronger than three others. This “strong” bond, assigned to patch 0, will result in the formation of

specific dimers that can be further ordered due to the weaker interactions encoded with patches 1, 2, and 3. For instance, let us consider a case in which patch  $A_0$  (i.e., the zeroth patch of particle  $A$ ) forms a strong bond with  $A^*_0$ , and there are similar strong bonds for other pairs:  $B_0-B^*_0, C_0-C^*_0$ , and  $D_0-D^*_0$ .

Once the four types of dimers are formed, we would like to arrange them into a diamond lattice. This is achieved as shown in Fig. 3(b): we start with a layer in which particles  $A, B, C$ , and  $D$  are arranged hexagonally, and then “program” assembly of the next hexagonal layer made of particles  $A^*, B^*, C^*$ , and  $D^*$  with a particular choice of pairwise interactions between patches. The advantage of this coloring scheme is that it uniquely defines the relative stacking of the two layers, the key for differentiating cubic and hexagonal diamonds (which have fcc- and hcp-type stacking, respectively). Note that each particle in our model can freely rotate about the bond axis. And yet, the  $D^*$  particle can only get bound to the  $A, B, C$  triad that is arranged clockwise, not counterclockwise. This uniquely selects one of the two possible stacking configurations. Now, recall that each particle is a part of a preformed dimer due to the “strong” bonding. This means that a new  $A, B, C, D$  layer is formed right on top  $A^*, B^*, C^*, D^*$ , essentially reproducing the starting arrangement, yet shifted to a new position. Obviously, if the procedure is repeated again, the layer will shift again by the same displacement vector. This corresponds to fcc-like stacking of  $A, B, C$ , and  $D$  particles and, hence, the cubic diamond arrangement of the whole structure.

How should the coloring of the patches be altered to encode hexagonal, rather than cubic, order? One might think that changing the particle chiralities would accomplish this. However, similarly to the honeycomb lattice in two dimensions, the monochiral system is consistent with exactly the same overall arrangement (CD), since at each step the new layer would simply switch to the alternative stacking, preserving the overall cubic symmetry. Instead, one can encode the hexagonal lattice by “rewiring” the strong bonds. If  $A_0$  is connected to  $B^*_0$ , and  $B_0$  to  $A^*_0$ , the newly formed  $B, A, C, D$  layer (on top of  $A^*, B^*, C^*, D^*$ ) will not be exactly the same as the original, shifted to a new position. All the clockwise and counterclockwise triangles in the lattice will switch chiralities. This means that one expects hexagonal (*ababab*) rather than cubic (*abcabc*) stacking of the layers in this case, yielding the HD structure.

### IV. RESULTS

To study the system, we use the force field introduced in our previous work [45]. The patch-patch pairwise interaction potentials are modeled as

$$V_{ij} = -\epsilon_{ij} \left( \frac{2a}{r} \right)^6 g(\theta_i) g(\theta_j). \quad (1)$$

Here  $\epsilon_{ij}$  is the interaction strength (in units of  $kT$ ) that depends on the patch colors,  $g(\theta) = [1 + e^{\alpha(\cos\theta_0 - \cos\theta)}]^{-1}$  is the angular potential, and  $\alpha = 124$  is its sharpness parameter. The angle  $\theta_i$  determines the orientation of patch  $i$  with respect to the centerline of the two particles, and  $\theta_0$  is its cutoff value

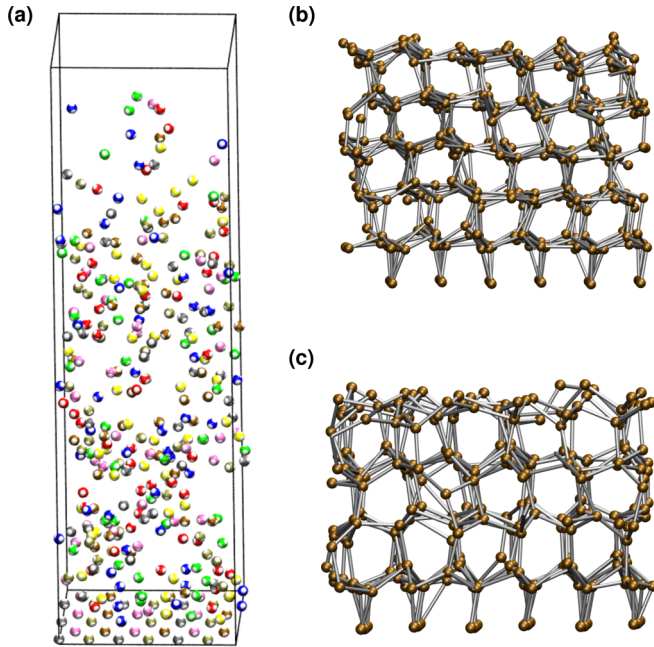


FIG. 4. Self-assembly of diamond using a surface template. (a) Snapshot of the simulation at the initial time. The template layer is made of 36 particles of types  $A^*$ ,  $B^*$ ,  $C^*$ , and  $D^*$ , which are fixed during the simulation. Self-assembled (b) cubic (426 particles) and (c) hexagonal diamond lattice (350 particles). Particle sizes are reduced, and bonds are explicitly indicated for a better visibility.

that determines the patch size. Other details of our model are given in Ref. [45].

We performed Brownian dynamics simulations for several versions of our system. First, we templated the self-assembly with a single prearranged hexagonal layer. We ran the simulations for two designs shown in Fig. 3, with a fixed number of particles, as shown in Fig. 4(a). The number of the particles in the templating layer was 36 (9 of each type). The simulation box had a rectangular base sized  $20.7a$  by  $18.1a$  to accommodate the templating layer, and its height was  $73a$ . The initial number of free particles of all types was  $N = 360$ , corresponding to the volume fraction of  $\Phi = 0.055$ .

While both CD and HD structures were formed as desired, the growth would eventually slow down due to depletion of the particles near the surface. To avoid this diffusion-limited regime, we modified the simulation protocol, effectively switching from the constant- $N$  to the constant chemical potential ensemble. Specifically, as the particles are bound to the surface, we replenish their supply by adding new particles at random positions inside the box, and keeping the overall number of free particles of each type fixed at  $N/8 = 45$ . This allowed us to grow bigger crystals, up to five layers, over much shorter simulation time (see Fig. 4). The assembly required approximately  $10^7$  time steps, which correspond to 500 in units of particle self-diffusion time. The quality of both CD and HD crystals grown in this way is exceptional: in a topological sense, they are 100% equivalent to the ideal cubic and hexagonal diamond lattices, respectively. Geometrically, they are of course deviating from the ideal crystal due to thermal fluctuations.

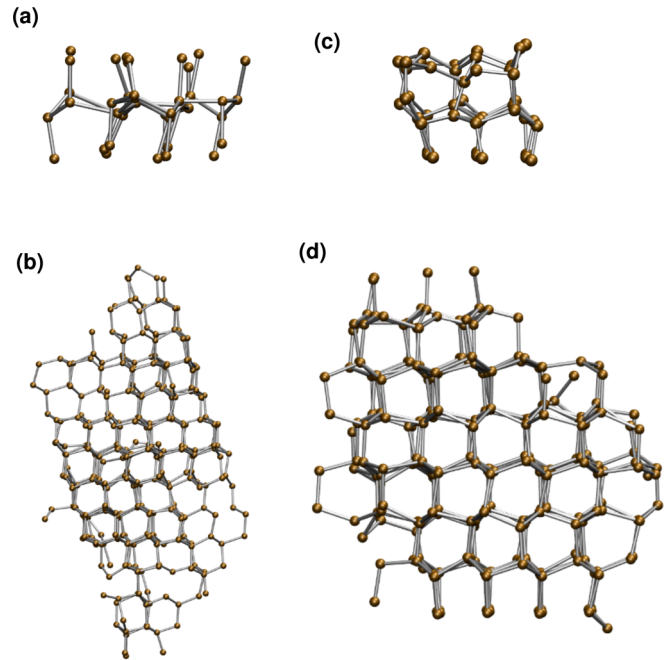


FIG. 5. Self-assembly of diamond from seeds: (a) CD seed used in simulation (40 particles), (b) self-assembled CD from seed (331 particles), (c) HD seed used in simulation (45 particles), and (d) self-assembled HD from seed (263 particles).

The interaction strength of the strong bonds was chosen large enough to ensure that they are effectively irreversible ( $\epsilon_{\text{strong}} = 20$ ). As for the weak bonds, the self-assembly was successful for a relatively broad range of their strengths:  $12 \leq \epsilon \leq 15$ . At greater values, the system shows random aggregation. Below, we observe a growing number of structural defects. The results are also not very sensitive to the patch size. Most of our simulations were performed for a patch angle of  $\theta_0 = 30^\circ$ , but we have also obtained ideal lattices for  $\theta_0 = 15^\circ$ . Systems with larger patches ( $\theta_0 = 40^\circ$ ) do not assemble into ordered structures (a patch this big would allow more than one particle to be bound to it).

In addition to the surface-templated crystal growth, we performed similar simulations starting with a small seed cluster of the respective structures, as shown in Fig. 5. Again, we were able to obtain near-perfect crystallites (up to thermal fluctuations) of the desired type, CD or HD. The seed size was systematically reduced until the minimal size needed for templating was achieved. This critical nucleus would typically contain about 40 particles. Naturally, the structure of the seed has to match the design of the system (cubic or hexagonal). Otherwise, no ordered structure has formed.

## V. DISCUSSION

In summary, we have successfully demonstrated a self-assembly of a desired diamond polymorph encoded with the help of chromatic patchy particles. An important aspect of the proposed scheme is its *robustness*: each added particle, once bound to three weak bonds, was guaranteed to occupy a correct spot. As a result, there was no need for multiparticle rearrangements to achieve the desired morphology. If our goal



FIG. 6. Schematic representation of the reduced-set, nonrobust design. It contains  $N = 6$  particle types, and  $K = 8$  bond types. Note that both stacking configurations are possible for  $B^*$  and  $C^*$  particles, but only one will eventually be selected (after rearrangements) due to the presence of  $A^*$ .

were just to ensure that the desired structure is the thermodynamic ground state, it could be accomplished with a smaller set of particles and patch colors. Specifically, Fig. 6 represents a modification of our original scheme that only contains three pairs of particle types. In this scheme, the threefold symmetry is restored for  $B^*$  and  $C^*$  particles; i.e., the weak bonds for each of these particles are indistinguishable. Hence,  $B^*$  and  $C^*$  particles do not contain information about the preferred stacking, and can bind to any  $ABC$  triangle, regardless of its chirality. However, particle  $A^*$  has all distinct patches and therefore can select the stacking for the whole layer. So, this system with  $N = 6$  (rather than 8) particle types and  $K = 8$  (rather than 16) bond types could also be programmed to assemble into CD or HD crystal, but it would not be robust. Instead, the domains with the two alternative layer stacking would form initially (as shown in Fig. 6), later relaxing to the desired one. This multiparticle process is significantly slower, and not achievable on the time scales of our simulations. However, this nonrobust scheme may still be feasible in certain experimental systems, especially at the nanoscale.

Our goal to achieve a robust design for error-free sequential assembly without slow multiparticle relaxation was a key reason behind introduction of “strong” bonds. As a result, instead of relying on individual particle binding sequentially, we had dimers as fundamental building blocks. When binding, individual particles would on average create two new contacts, while the dimers create three. Hence, the dimer, once bound with three correct bonds, is guaranteed to occupy a correct location in space, which would not be the case with single particles. As expected, a system in which all four bonds have

the same strength does not form ordered structure in our simulations. This certainly does not rule out that ordering could be achieved via the multiparticle relaxation mechanism, on a much longer time scale than those probed in our studies. Similarly, the runtime was not long enough to observe spontaneous nucleation of the crystal, and we used the preformed seeds instead. Nevertheless, our results allow one to estimate the size of the critical nucleus as approximately 40 particles (or 20 dimers). It is larger than those found in MC studies of the DNA brick model [17,18]. However, since the actual building blocks in our system are dimers rather than single particles, a more reasonable reference model for our case should be patchy particles with coordination number 6 rather than 4. In that case, MC simulations show a significantly larger critical nucleus, consistent with our result for 20 dimers [46]. Note that those MC studies of nucleation effectively complement our own results, since our prime focus was on the growth kinetics and quality of the resulting system. Another approach that provides a perfect complement to ours is a recent proposal of solving the inverse self-assembly problem as an optimization problem in the parameter space (specifically, for various 2D structures) in Ref. [47]. An important distinction is that our central goal was to optimize the kinetic pathway rather than to make sure that the target structure is indeed a preferred equilibrium state.

Finally, we would like emphasize the generic nature of our findings. As we discussed earlier, the patchy particle model, originally introduced to describe molecular-scale phenomena, has been revitalized due to its relevance for engineered colloidal systems. However, its applicability is much broader. It naturally applies to NPs directionally functionalized with DNA [14,15,43], to DNA cages and “caged” particles [16,36,42], to DNA constructs in the context of the DNA brick model [17,18,40], to the self-assembly of proteins [48,49], and beyond. This opens up the possibility of applying the same ideas for various platforms on different length scales. For instance, our design can be directly tested with the help of existing nanoscale techniques, such as DNA-caged NPs. This would be an excellent model system to facilitate future progress in microscopic patchy colloids. The recent advances in DNA-mediated NP and colloidal self-assembly can serve as an inspiration on how progress made on one length scale can boost development on another [1–4].

#### ACKNOWLEDGMENTS

This research was carried out at Center for Functional Nanomaterials, which is a U.S. DOE Office of Science Facility, at Brookhaven National Laboratory under Contract No. DE-SC0012704, and used resources from the Scientific Data and Computing Center, a component of the Computational Science Initiative.

[1] D. Nykypanchuk, M. M. Maye, D. van der Lelie, and O. Gang, *Nature (London)* **451**, 549 (2008).

[2] S. Y. Park, A. K. R. Lytton-Jean, B. Lee, S. Weigand, G. C. Schatz, and C. A. Mirkin, *Nature (London)* **451**, 553 (2008).

- [3] R. J. Macfarlane, B. Lee, M. R. Jones, N. Harris, G. C. Schatz, and C. A. Mirkin, *Science* **334**, 204 (2011).
- [4] Y. Wang, Y. Wang, X. Zheng, E. Ducrot, J. S. Yodh, M. Weck, and D. J. Pine, *Nat. Commun.* **6**, 7253 (2015).
- [5] A. V. Tkachenko, *Phys. Rev. Lett.* **89**148303 (2002).
- [6] F. J. Martinez-Veracoechea, B. M. Mladek, A. V. Tkachenko, and D. Frenkel, *Phys. Rev. Lett.* **107**, 045902 (2011).
- [7] W. B. Rogers, W. M. Shih, and V. N. Manoharan, *Nat. Rev. Mater.* **1**, 8 (2016).
- [8] V. Manoharan, M. Elsesser, and D. Pine, *Science* **301**, 483 (2003).
- [9] Y. Wang, Y. Wang, D. Breed, V. Manoharan, L. Feng, A. Hollingsworth, M. Weck, and D. Pine, *Nature (London)* **491**, 51 (2012).
- [10] F. Romano, E. Sanz, and F. Sciortino, *J. Chem. Phys.* **132**, 184501 (2010).
- [11] E. Bianchi, J. Largo, P. Tartaglia, E. Zaccarelli, and F. Sciortino, *Phys. Rev. Lett.* **97**, 168301 (2006).
- [12] Z. L. Zhang and S. C. Glotzer, *Nano Lett.* **4**, 1407 (2004).
- [13] A. B. Pawar and I. Kretschmar, *Macromol. Rapid Commun.* **31**, 150 (2010).
- [14] A. V. Tkachenko, *Phys. Rev. Lett.* **106**, 255501 (2011).
- [15] J. D. Halverson and A. V. Tkachenko, *Phys. Rev. E* **87**, 062310 (2013).
- [16] W. Liu, J. Halverson, Y. Tian, A. Tkachenko, and O. Gang, *Nat. Chem.* **8**, 867 (2016).
- [17] A. Reinhardt and D. Frenkel, *Phys. Rev. Lett.* **112**, 238103 (2014).
- [18] A. Reinhardt and D. Frenkel, *Soft Matter* **12**, 6253 (2016).
- [19] O. A. Vasilyev, B. A. Klumov, and A. V. Tkachenko, *Phys. Rev. E* **92**, 012308 (2015).
- [20] K. M. Ho, C. T. Chan, and C. M. Soukoulis, *Phys. Rev. Lett.* **65**, 3152 (1990).
- [21] E. Yablonovitch, T. J. Gmitter, and K. M. Leung, *Phys. Rev. Lett.* **67**, 2295 (1991).
- [22] M. Maldovan and E. L. Thomas, *Nat. Mater.* **3**, 593 (2004).
- [23] J. Kolafa and I. Nezbeda, *Mol. Phys.* **61**, 161 (1987).
- [24] L. Feng, R. Dreyfus, R. J. Sha, N. C. Seeman, and P. M. Chaikin, *Adv. Mater.* **25**, 2779 (2013).
- [25] F. Sciortino, E. Bianchi, J. F. Douglas, and P. Tartaglia, *J. Chem. Phys.* **126**, 2730797 (2007).
- [26] J. Russo, J. M. Tavares, P. I. C. Teixeira, M. M. Telo da Gama, and F. Sciortino, *Phys. Rev. Lett.* **106**, 085703 (2011).
- [27] J. M. Tavares, P. I. C. Teixeira, and M. M. T. da Gama, *Mol. Phys.* **107**, 453 (2009).
- [28] D. de las Heras, J. M. Tavares, and M. M. T. da Gama, *J. Chem. Phys.* **134**, 3561396 (2011).
- [29] F. Romano, E. Sanz, and F. Sciortino, *J. Chem. Phys.* **134**, 3578182 (2011).
- [30] E. Bianchi, G. Doppelbauer, L. Filion, M. Dijkstra, and G. Kahl, *J. Chem. Phys.* **136**, 4722477 (2012).
- [31] F. Romano and F. Sciortino, *Nat. Commun.* **3**, 975 (2012).
- [32] F. Smallenburg and F. Sciortino, *Nat. Phys.* **9**, 554 (2013).
- [33] Z. L. Zhang, A. S. Keys, T. Chen, and S. C. Glotzer, *Langmuir* **21**, 11547 (2005).
- [34] O. A. Vasilyev, B. A. Klumov, and A. V. Tkachenko, *Phys. Rev. E* **88**, 012302 (2013).
- [35] E. G. Noya, C. Vega, J. P. K. Doye, and A. A. Louis, *J. Chem. Phys.* **132**, 3454907 (2010).
- [36] W. Liu, M. Tagawa, H. L. Xin, T. Wang, H. Emamy, H. Li, K. G. Yager, F. W. Starr, A. V. Tkachenko, and O. Gang, *Science* **351**, 582 (2016).
- [37] Y. Wang, I. C. Jenkins, J. T. McGinley, T. Sinno, and J. C. Crocker, *Nat. Commun.* **8**, 14173 (2017).
- [38] A. P. Hynninen, J. H. J. Thijssen, E. C. M. Vermolen, M. Dijkstra, and A. Van Blaaderen, *Nat. Mater.* **6**, 202 (2007).
- [39] T. Dasgupta and M. Dijkstra, *Soft Matter* **14**, 2465 (2018).
- [40] W. M. Jacobs and D. Frenkel, *J. Am. Chem. Soc.* **138**, 2457 (2016).
- [41] Y. G. Ke, L. L. Ong, W. M. Shih, and P. Yin, *Science* **338**, 1177 (2012).
- [42] N. A. Licata and A. V. Tkachenko, *Phys. Rev. E* **79**, 011404 (2009).
- [43] T. Trinh, C. Y. Liao, V. Toader, M. Barlog, H. S. Bazzi, J. N. Li, and H. F. Sleiman, *Nat. Chem.* **10**, 184 (2018).
- [44] X. Zheng, Y. Wang, Y. Wang, D. Pine, and M. Weck, *Chem. Mater.* **28**, 3984 (2016).
- [45] N. Patra and A. V. Tkachenko, *Phys. Rev. E* **96**, 022601 (2017).
- [46] A. Reinhardt, C. P. Ho, and D. Frenkel, *Faraday Discuss.* **186**, 215 (2016).
- [47] D. Chen, G. Zhang, and S. Torquato, *J. Phys. Chem. B*, **122**, 8462 (2018).
- [48] D. Fusco and P. Charbonneau, *Phys. Rev. E* **88**, 012721 (2013).
- [49] D. Fusco and P. Charbonneau, *Colloids Surf. B* **137**, 22 (2016).